Thick-to-Thin Filament Surface Distance Modulates Cross-Bridge Kinetics in *Drosophila* Flight Muscle

Bertrand C. W. Tanner,[†] Gerrie P. Farman,[‡] Thomas C. Irving,[§] David W. Maughan,[†] Bradley M. Palmer,[†] and Mark S. Miller[†*]

[†]Department of Molecular Physiology and Biophysics, University of Vermont, Burlington, Vermont; [‡]Department of Physiology and Biophysics, Boston University, Boston, Massachusetts; and [§]Center for Synchrotron Radiation Research and Instrumentation, Department of Biological and Chemical Sciences, Illinois Institute of Technology, Chicago, Illinois

ABSTRACT The demembranated (skinned) muscle fiber preparation is widely used to investigate muscle contraction because the intracellular ionic conditions can be precisely controlled. However, plasma membrane removal results in a loss of osmotic regulation, causing abnormal hydration of the myofilament lattice and its proteins. We investigated the structural and functional consequences of varied myofilament lattice spacing and protein hydration on cross-bridge rates of force development and detachment in *Drosophila melanogaster* indirect flight muscle, using x-ray diffraction to compare the lattice spacing of dissected, osmotically compressed skinned fibers to native muscle fibers in living flies. Osmolytes of different sizes and exclusion properties (Dextran T-500 and T-10) were used to differentially alter lattice spacing and protein hydration. At in vivo lattice spacing, cross-bridge attachment time (t_{on}) increased with higher osmotic pressures, consistent with a reduced cross-bridge detachment rate as myofilament protein hydration decreased. In contrast, in the swollen lattice, t_{on} decreased with higher osmotic pressures. These divergent responses were reconciled using a structural model that predicts t_{on} varies inversely with thick-to-thin filament surface distance, suggesting that cross-bridge rates of force development and detachment are modulated more by myofilament lattice geometry than protein hydration. Generalizing these findings, our results suggest that cross-bridge cycling rates slow as thick-to-thin filament surface distance decreases with sarcomere lengthening, and likewise, cross-bridge cycling rates increase during sarcomere shortening. Together, these structural changes may provide a mechanism for altering cross-bridge performance throughout a contraction-relaxation cycle.

INTRODUCTION

Cell volume, osmolarity, hydration, and ion activity are exquisitely regulated by the plasma membrane to maintain proper cellular function (1,2). Removing or damaging the plasma membrane disrupts the osmotic and ionic balances, thereby altering the conformation and activity of the intracellular enzymes (3,4). Single demembranated (skinned) muscle fibers are widely used to investigate contractility at the molecular level because removal of the sarcolemma allows precise control and manipulation of the intracellular ionic conditions. However, intracellular osmolytes diffuse out of the skinned fiber as the endogenous fluid medium equilibrates with the exogenous skinning solution. The accompanying reduction in intracellular osmotic pressure results in expansion and hydration of the myofilament lattice and proteins (5–8). These changes in myofilament spacing and protein hydration may alter cross-bridge kinetics and force generation, confounding the interpretation of skinned fiber studies.

The osmotic influence of an intact sarcolemma can be mimicked in skinned muscle fibers by adding large, neutral, long-chain polymers (e.g., Dextran T-500; 500 kDa) to the bathing solution. These high molecular mass polymers remain excluded from the myofilament lattice (7,8), thereby providing an osmotic pressure that decreases myofilament lattice spacing as water is drawn out of the fiber. Adding 4–6% w/v Dextran T-500 to the bathing solution compresses skinned fibers to their in vivo lattice spacing (7–10) and decreases the rate of force development and cross-bridge cycling roughly 10–20% in both vertebrates and invertebrates (10–13). These results show that structural changes in the myofilament lattice can alter cross-bridge performance. Overall, these previous studies support the notion that osmotic compression sterically alters cross-bridge movement due to reduced lattice spacing, thereby decreasing cross-bridge cycling rates (7,8,11,12). However, the previous studies did not address whether osmotic compression dehydrates myofilament proteins as water is drawn out of the myofilament lattice, as suggested by the reductions in thick filament diameter due to osmotic compression from Dextran T-200 and T-2000 (14). Therefore, reduced myofilament protein hydration represents a biophysical perturbation that could independently alter cross-bridge rates of force development and detachment. Low molecular mass polymers that freely diffuse into the myofilament lattice space (e.g., Dextran T-10 (10 kDa) and polyethylene glycol (PEG, 0.3–4 kDa)) have been shown to reduce myofilament protein hydration without significantly changing myofilament lattice spacing (15–17). Reduced protein hydration elicited a variety of cross-bridge behaviors, from no change in the rates of force development and detachment for skinned fiber (13) or solution ATPase measurements (17) at modest

Submitted May 21, 2012, and accepted for publication August 6, 2012.

*Correspondence: Mark.Miller@uvm.edu

Editor: Shin'ichi Ishiwata.

0006-3495/12/09/1275/10 $2.00

http://dx.doi.org/10.1016/j.bpj.2012.08.014

osmotic pressures (i.e., the ~3 kPa required to return in vivo spacing, Fig. 1), to increasingly slowed cross-bridge cycling rates with further increases in osmotic pressure (15,16). Altogether, these previous studies show that both altered myofilament spacing and protein hydration play important roles in dictating cross-bridge transition rates, although their relative contributions remain unclear, particularly at or near in vivo osmotic conditions.

To investigate the structural and functional consequences of varied myofilament spacing and protein hydration, we returned these parameters to their in vivo values in skinned *Drosophila melanogaster* indirect flight muscle (IFM) by osmotic compression with Dextran T-500 or T-10 and measured myosin-actin cross-bridge kinetics via sinusoidal length perturbation analysis. The use of *Drosophila* is an important aspect of this study, as x-ray diffraction (XRD) can be used to compare the lattice spacing of native, hydrated muscle in living flies to the lattice spacing of osmotically compressed single fibers (10). Using spacing values measured from the x-ray data in combination with muscle mechanics, we examined the functional consequences of matching inter-thick filament spacing or myofilament protein hydration. These empirical results and a structural model of myofilament organization indicate that the frequency of maximal power production and cross-bridge attachment time (t_{on}) are linearly correlated with thick-to-thin filament surface distance. Although changes in myofilament protein hydration affected cross-bridge rates of force development and detachment, these rates were more greatly influenced by variations in myofilament lattice geometry.

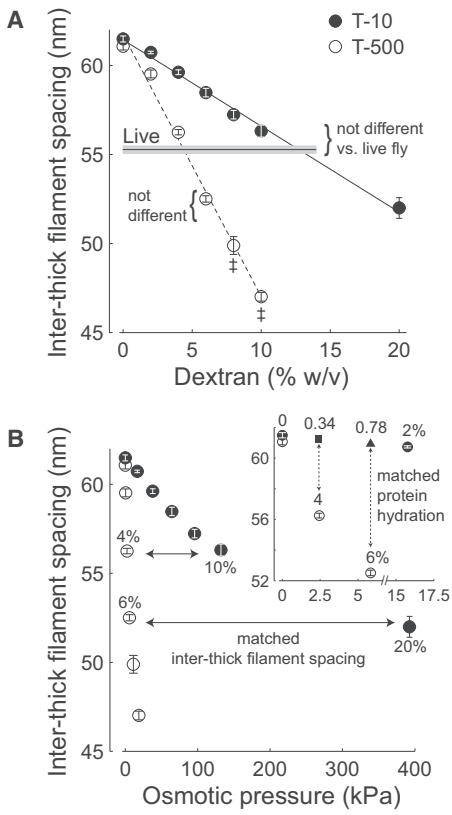

FIGURE 1 Center-to-center inter-thick filament spacing of IFM from resting, live flies, or skinned, relaxed fibers compressed with T-500 or T-10 plotted against Dextran concentration (*A*) or osmotic pressure (*B*). In panel *A*, the horizontal line bounded by gray shading depicts the mean ± SE of the live fly measurements ($n = 16$), while symbols depict skinned single fiber measurements for T-500 ($n = 17$–22) or T-10 ($n = 6$–10). Linear fits to the mean values at each Dextran concentration are depicted by a dashed line for T-500 (slope = -1.47 nm $\%^{-1}$, intercept = 61.73) or a solid line for T-10 (slope = -0.48 nm $\%^{-1}$, intercept = 61.42 nm). In panel *B*, horizontal, solid arrows highlight Dextran concentrations that produce matched inter-thick filament spacing (4% vs. 10% and 6% vs. 20% for T-500 vs. T-10, respectively), while vertical, dashed arrows highlight Dextran concentrations that produce similar myofilament protein hydration at matched osmotic pressures (*inset*, 4% vs. 0.34% and 6% vs. 0.78% for T-500 vs. T-10, respectively). Inter-thick filament spacing values for 0.34% and 0.78% T-10 were interpolated from the linear fit in panel *A*, shown with different symbols than measured spacing values (*inset*, panel *B*).

MATERIALS AND METHODS

Experimental methods are summarized below. Additional details about solution composition, XRD, muscle mechanics, and statistical analysis are presented in the Supporting Material.

Solutions

Solutions were prepared as previously described (10) for XRD and muscle mechanics. Dextran T-500 or T-10 (Pharmacosmos, Holbaek, Denmark) were added at varied concentrations (c, in % w/v) and osmotic pressure (Π, in kPa) was calculated from measured pressure-concentration relationships for T-500 (18) or T-10 (8):

$$\Pi(c) = A_1 c + A_2 c^2 + A_3 c^3, \quad (1)$$

with virial coefficients (A_i, units kPa $\%^{-i}$) of $A_1 = 0.0664$, $A_2 = 0.1051$, and $A_3 = 0.0076$ for T-500 and $A_1 = 7.05$, $A_2 = 0.6060$, $A_3 = 0.0012$ for T-10. We assume Dextran T-500 is fully excluded from the myofilament lattice and Dextran T-10 freely enters the myofilament lattice. This assumption follows from previous observations using Dextran T-40 (8), which indicate polymer fractions of molecular mass <20 kDa enter the lattice and >20 kDa are excluded from the lattice. The mass percent of T-500 <20 kDa and of T-10 >20 kDa are negligibly small (<2%), according to the manufacturer's data.

As Dextran T-500 is excluded from the myofilament lattice, T-500 must be excluded from the myofilaments. Previous modeling of XRD data from relaxed skinned skeletal muscle fibers of the frog confirm thick filaments can be compressed by Dextran T-200 and T-2000 (14), which are excluded from the myofilament lattice (19). The myofilaments (each a tightly knit assembly of myosin or actin and accessory proteins) most likely exclude Dextran T-10, except for the lowest mass molecular fractions. Water molecules, metal ions, and small metabolites are expected to penetrate the myofilaments, as they do the lattice. However, the Gibbs dividing surface that defines the interface between the myofilaments and bathing medium (20), is indistinct, even if the three-dimensional myofilament structure is known with precision, because the location of this hypothetical surface differs with solute size. Thus, the degree of T-10 exclusion from the myofilaments cannot be readily calculated. Given the similarity in degree of polymer exclusion at the filament level, we assumed that matched osmotic pressures between Dextran T-500 and T-10 produce similar myofilament

protein hydration conditions (20). This general assumption is supported by DNA studies that show a given increase in osmotic pressure leads to an identical change in chemical potential of water, independent of the identity of the stressing polymer (21). In other words, we assume that the amount of water contained within the myofilament proteins, such as myosin or the thick filament, will be the same under equivalent osmotic pressures produced by T-500, which remains outside the myofilament lattice, or by T-10, which penetrates the myofilament lattice.

X-ray diffraction (XRD)

XRD measurements were obtained using the small angle instrument on the Biophysics Collaborative Access Team (BioCAT) beamline at the Advanced Photon Source (Argonne, IL) as previously described for resting, live *Drosophila melanogaster* (22,23), and skinned IFM fibers (10). Solution exchanges on individual fibers were performed at increasing Dextran concentrations for either T-500 or T-10 (2, 4, 6, 8, 10% T-500 or 2, 4, 6, 8, 10, 20% T-10). All XRD measurements occurred at room temperature (22°C).

Muscle mechanics

Mechanical measurements and curve fitting were carried out as in previous studies (10,24). Activating solutions with increasing Dextran concentrations were exchanged to obtain 4 and 6% T-500 or 0.34, 0.78, 10, and 20% T-10. Because inter-thick filament spacing decreases only slightly (~0.8%) from relaxed to full activated conditions in wild-type (WT) flies (22), we expect no differences in the amount of Dextran required to compress skinned fibers back to in vivo spacing values between relaxed and active conditions. Solutions were maintained at 15°C.

Sinusoidal analysis consisted of small amplitude sinusoidal length changes (L_A = 0.125% muscle length) applied at discrete frequencies (0.5–1000 Hz), while measuring the tensile stress (force divided by fiber cross-sectional area) and strain (change in muscle length divided by the original fiber length) from the activated muscle fibers. Digital Fourier transforms were applied to the measured stress and strain signals to calculate the complex modulus ($Y(\omega)$, where ω is angular frequency) from the quotient of these digital Fourier transforms (stress/strain). Elastic and viscous moduli (kN m^{-2}) are defined as the in-phase and out-of-phase portions of complex modulus, respectively. Specific work (J m^{-3}) and power (W m^{-3}) over a single oscillatory cycle are proportional to viscous modulus (E_v), where work = $-E_v\pi L_A^2$ and power = $-E_v L_A^2\omega/2$.

For our analysis to estimate cross-bridge rate constants, the force response must remain linear, which requires small amplitude length changes (L_A = 0.125%). The large amplitude perturbations of work-loop analysis, meant to mimic in vivo shortening and lengthening, place large stresses and strains on the cross-bridges and myofilaments, which leads to a nonlinear force response that is difficult to relate to cross-bridge rates of force development and detachment. As maximal work and power production scale with L_A^2, oscillatory work production from sinusoidal analysis generally remains less than values measured using work-loop analysis (L_A = 0.75–1.5% muscle length) (25).

The complex modulus (plotted as viscous versus elastic modulus) was characterized, or fit, by

$$Y(\omega) = A(i\omega)^k - B\left(\frac{i\omega}{2\pi b + i\omega}\right) + C\left(\frac{i\omega}{2\pi c + i\omega}\right), \quad (2)$$

and provides estimates for model parameters: A, k, B, b, C, and c. Magnitude parameters A, B, and C (kN m^{-2}) are related to stress produced by the fiber, whereas the characteristic frequencies b and c (Hz) are related to cross-bridge cycling rates. The exponential parameter k (unitless, range 0–1) describes the degree to which measured viscoelastic mechanics represent purely elastic (k = 0) versus purely viscous (k = 1) mechanical responses. The A-process reflects viscoelastic properties of structural elements within the fiber. Enzymatic cross-bridge cycling during Ca^{2+}-activated contraction produces frequency dependent shifts in the viscous and elastic moduli represented by B- and C-processes to characterize work producing (cross-bridge recruitment) and absorbing (cross-bridge distortion) processes (13,26,27). The characteristic frequency b is correlated with the observed rate of myosin force production and scales proportionally with shifts in the frequency of maximal oscillatory work and power output (13), whereas c is related to the cross-bridge detachment rate (and inversely related to the mean duration of cross-bridge attachment: $t_{on} = (2\pi c)^{-1}$ (27)).

Statistical analysis

All values are mean ± SE. Constrained nonlinear least squares fitting of Eq. 2 to complex moduli was performed using a sequential quadratic programming method in MATLAB (v 7.9.0, The MathWorks, Natick, MA). Statistical analyses were considered significant at $p < 0.05$ and were performed using SPSS (v.16.0, SPSS, Chicago, IL) and MATLAB.

RESULTS

X-ray diffraction (XRD)

Center-to-center inter-thick filament spacing of the IFM from resting, live flies was 55.3 ± 0.2 nm (Fig. 1). After skinning, inter-thick filament spacing of single IFM fibers in relaxing solution without Dextran increased 10–11% compared to the live fly value, as previously observed (10). Inter-thick filament spacing of single fibers decreased with increasing Dextran T-500 or T-10 concentration (Fig. 1 *A*). The reduction in inter-thick filament spacing with increased Dextran concentration was roughly three times greater for T-500 than for T-10, illustrated by the larger slope of the linear fits to these data for T-500.

Inter-thick filament spacing was also plotted against calculated osmotic pressure (Eq. 1, Fig. 1 *B*), showing that T-500 reduced lattice spacing more than T-10 at identical pressures. For instance, 4% T-500 and 10% T-10 compressed inter-thick filament spacing to in vivo dimensions (Fig. 1 *B*, *horizontal arrows*), but the corresponding osmotic pressures were roughly 50 times different (2.4 kPa for 4% T-500 versus 132.3 kPa for 10% T-10). T-500 concentrations that compressed inter-thick filament spacing back to (4%) and slightly beyond (6%) in vivo values were selected for single fiber mechanics. T-10 concentrations were selected by matching inter-thick filament spacing (10% and 20%) and osmotic pressure, or protein hydration (0.34% and 0.78%), with the T-500 (4% and 6%) concentrations.

Skinned muscle fiber mechanics

Our primary measures of oscillatory power output and the model parameters are calculated from the elastic (EM) and viscous (VM) moduli. The frequency responses of EM and VM did not differ between T-500 and T-10 in the absence of Dextran (Fig. 2, *A* and *D*). Reducing the swollen myofilament lattice to in vivo spacing using 4% T-500 (Fig. 1) shifted the EM and VM to lower frequencies

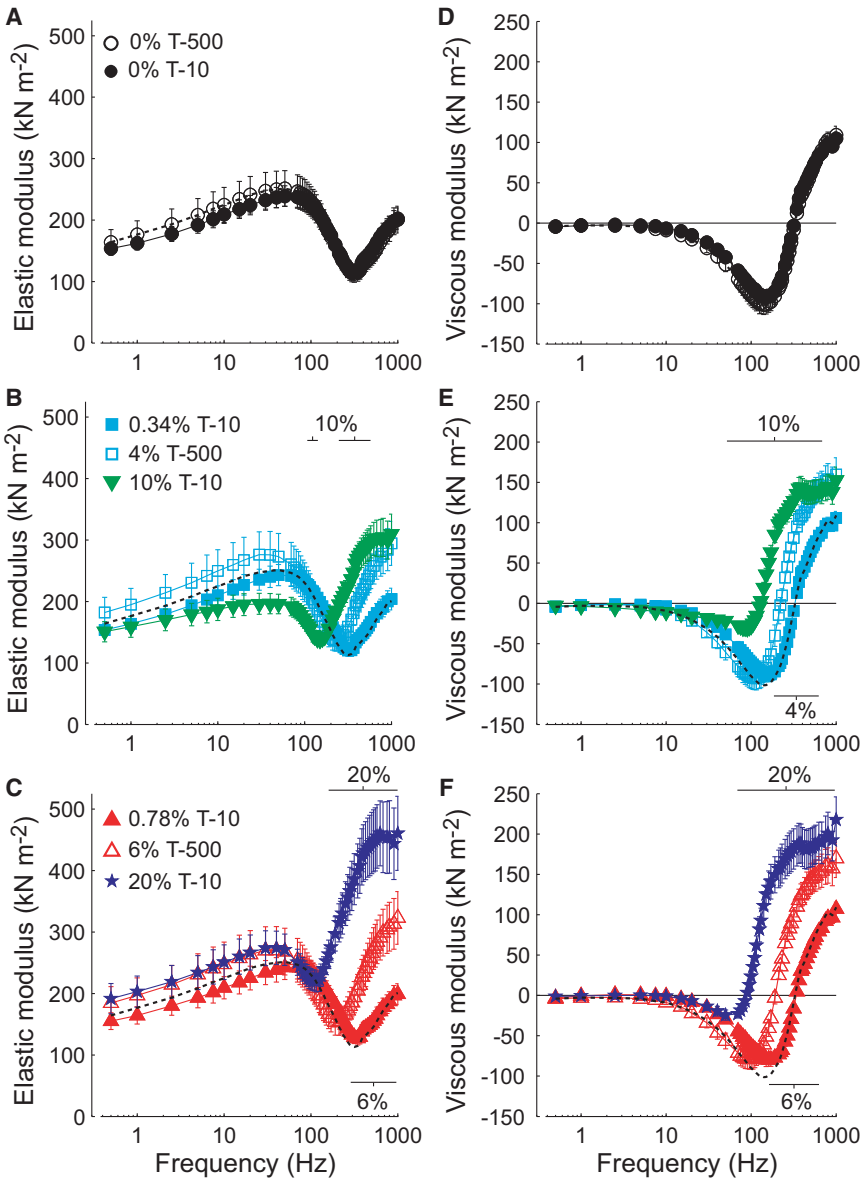

FIGURE 2 Elastic and viscous moduli from Ca^{2+}-activated (pCa 4.5) skinned IFM fibers in the absence and presence of Dextran T-500 or T-10 (*n* in Table 1) are plotted against sinusoidal oscillatory frequency. (*A* and *D*) Moduli in the absence of Dextran (larger inter-thick filament lattice spacing values compared to in vivo). (*B* and *E*) Moduli at 4% T-500 (in vivo inter-thick filament spacing), 0.34% T-10 (matched osmotic pressure with 4% T-500) and 10% T-10 (matched spacing with 4% T-500). (*C* and *F*) Moduli at 6% T-500 (slightly smaller than in vivo spacing), 0.78% T-10 (matched osmotic pressure with 6% T-500), and 20% T-10 (matched spacing with 6% T-500). Black dashed lines denoting the 0% T-500 condition are replotted on panels *B*, *C*, *E*, and *F*. Horizontal bars indicate frequencies that are significantly different at the given Dextran concentration from 0% T-500. Horizontal solid lines depict zero viscous modulus (*D–F*), signifying the transition between work absorbing (positive viscous moduli) and work producing (negative viscous moduli) mechanical behavior.

compared to 0% (Fig. 2, *B* and *E*), indicating slowed rates of cross-bridge cycling. Adding 0.34% T-10 matched the myofilament protein hydration of 4% T-500 and produced a small shift to higher frequencies in the EM and VM compared to 0% (Fig. 2, *B* and *E*), indicating increased rates of cross-bridge cycling. As shown in Fig. 1, 10% T-10 and 4% T-500 compressed the myofilament lattice to in vivo spacing, but required roughly 50 times the osmotic pressure for T-10 compared to T-500. Although lattice spacing was similar for these two conditions, the EM and VM frequency responses were shifted to lower frequencies for 10% T-10 than for 4% T-500 (Fig. 2, *B* and *E*).

Similar, but larger shifts in the frequency response were found with higher osmotic compressions (Fig. 2, *C* and *F*). The addition of 6% T-500 reduced myofilament lattice spacing below the in vivo value, shifting EM and VM to even lower frequencies than 4% T-500. At 0.78% T-10, or matched myofilament protein hydration with 6% T-500, EM and VM shifted to higher frequencies compared to 0.34% and 0%, although were not statistically different from 0% at any specific frequency. At 20% T-10, or matched lattice spacing with 6% T-500, the EM and VM frequency responses were shifted to lower frequencies for 20% T-10 than for 6% T-500.

No significant differences were found in Ca^{2+} activated oscillatory power output between T-500 and T-10 at 0% Dextran (Fig. 3 *A*). Adding 4% T-500 (in vivo lattice spacing) reduced the maximal power and frequency of maximal power by 26–30% compared to 0% (Fig. 3 *B*, Table 1). Adding 0.34% T-10 matched the myofilament protein hydration of 4% T-500, but shifted the power-frequency relationship to higher frequencies compared to 0%, without affecting the

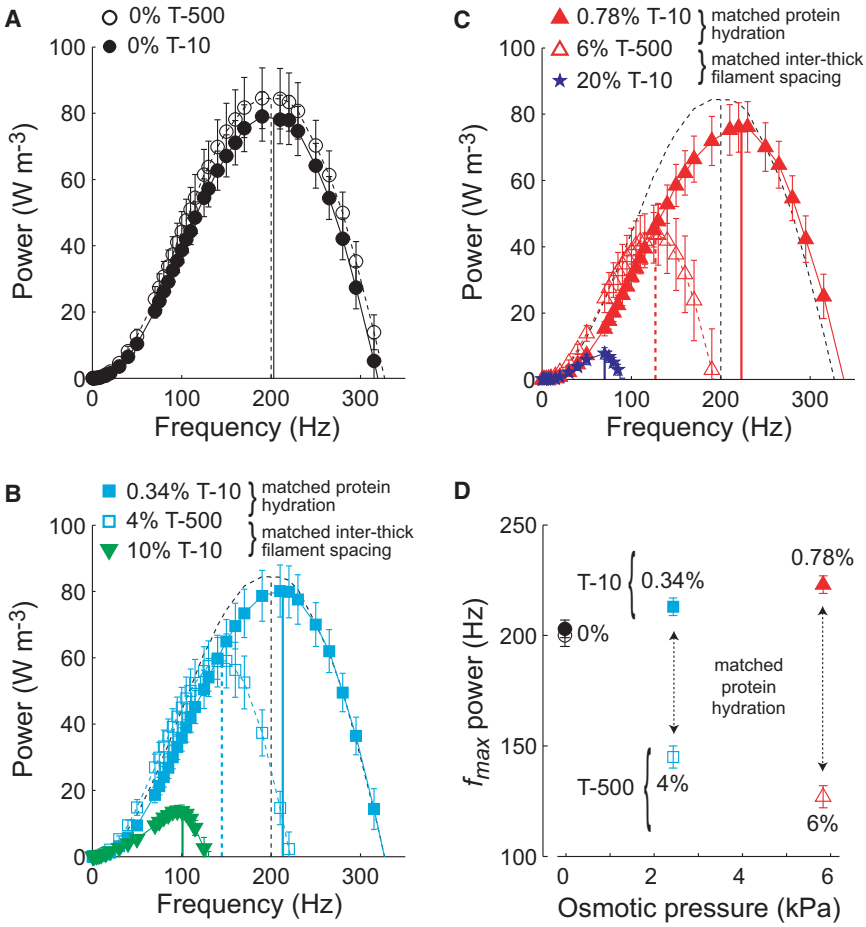

FIGURE 3 Oscillatory power output from Ca^{2+}-activated (pCa 4.5) skinned IFM fibers in the absence and presence of Dextran T-500 or T-10 (n in Table 1) are plotted against sinusoidal oscillation frequency. (*A*) Power in the absence of Dextran (inter-thick filament lattice spacing swollen compared to in vivo). (*B*) Power at 4% T-500 (in vivo inter-thick filament spacing), 0.34% T-10 (matched osmotic pressure with 4% T-500), and 10% T-10 (matched spacing with 4% T-500). (*C*) Power at 6% T-500 (slightly smaller than in vivo spacing), 0.78% T-10 (matched osmotic pressure with 6% T-500), and 20% T-10 (matched spacing with 6% T-500). (*D*) At modest osmotic pressures, the frequency at which maximal power output occurs (f_{max} power) increases for T-10 and decreases for T-500 compared to the 0% value. For panels *A–C*, vertical lines illustrate f_{max} power for each condition. Black dashed lines denoting the power output and f_{max} power for the 0% T-500 condition are replotted on panels *B* and *C*.

magnitude of maximal power output. At 10% T-10 and 4% T-500 the myofilament lattice spacing equals in vivo, but the maximal power and frequency of maximal power were decreased more for 10% T-10 (50–80%) than for 4% T-500 (27–28%), compared to 0%. Additional osmotic compression with 6% T-500 and 20% T-10 reduced myofilament lattice spacing below the in vivo value, shifting oscillatory power output to even lower frequencies and further reduced maximal power output (Fig. 3 *C*). In contrast, at conditions of matched myofilament protein hydration (6% T-500 and 0.78% T-10), 0.78% T-10 shifted oscillatory power output to greater frequencies than 0% without a significant change in maximal power output. The frequency and magnitude of oscillatory work production followed trends similar to oscillatory power output, with subtle differences in the sensitivity to varied Dextran concentrations (Table 1).

These data indicate divergent trends for the effect of T-500 versus T-10 on the frequency of maximal power output at

TABLE 1 Frequency and magnitude of maximal power output and work production (mean ± SE)

Dextran concentration	Osmotic pressure	Maximal power		Maximal work		
(wt/vol)	(kPa)	(W m^{-3})	f_{max} (Hz)	(J m^{-3})	f_{max} (Hz)	(n)
0% T-500	0	86 ± 9	200 ± 5	0.51 ± 0.06	143 ± 6	11
4% T-500	2.44	63 ± 11*†	145 ± 5*†‡	0.47 ± 0.07	112 ± 3*†	11
6% T-500	5.83	46 ± 8*†	127 ± 5*†‡	0.39 ± 0.06*†	100 ± 3*†	11
0% T-10	0	80 ± 8	203 ± 4	0.45 ± 0.04	155 ± 4	12
0.34% T-10	2.44	81 ± 8	213 ± 4	0.44 ± 0.04	157 ± 3	12
0.78% T-10	5.83	78 ± 8	223 ± 4*	0.39 ± 0.04	164 ± 5	10
10% T-10	132.25	15 ± 2*†	99 ± 3*†‡	0.16 ± 0.02*	90 ± 3*†	12
20% T-10	392.6	8 ± 2*†	70 ± 2*†‡	0.13 ± 0.03*	58 ± 3*†‡	12

*Differs from 0% Dextran value within the population of T-10 or T-500 measurements using a linear mixed model with Dextran concentration as the repeated measure followed by a pairwise comparison of the means ($p < 0.05$).
†Differs from all other values within the population of T-10 or T-500 measurements using a linear mixed model with Dextran concentration as the repeated measure followed by a pairwise comparison of the means ($p < 0.05$).
‡Differs from all other values among the entire population of measurements using a 1-way ANOVA followed by a multiple comparison of means ($p < 0.05$).

modest pressures flanking the estimated in vivo lattice spacing (Fig. 3 *D*). Because lower versus higher shifts in the frequency response of power output correspond to decreased versus increased cross-bridge cycling rates, these measurements consistently demonstrate slowed cross-bridge cycling with reduced inter-thick filament spacing. In addition, matched inter-thick filament spacing values at larger osmotic pressures (4% vs. 10% and 6% vs. 20% for T-500 vs. T-10) further decreased the power output frequencies, indicating slower cross-bridge cycling as myofilament protein hydration decreased. In contrast, comparing 0% and 0.78% T-10, the frequency of maximal power output increased, suggesting faster cross-bridge cycling as myofilament protein hydration decreased at lattice spacings larger than in vivo.

The widespread similarities among the A-processes (*A* and *k*) and magnitudes of the B- and C-processes (*B* and *C*) for all Dextran conditions show little or no difference in the cross-bridge's capability of binding actin and generating force with altered Dextran concentrations (Table 2). In contrast, striking differences arose from the characteristic frequency parameters *b* and *c*. The B-process arises from work-producing processes during active muscle contraction, with larger *b* values indicating faster cross-bridge rates of force production (13). The C-process arises from work-absorbing processes during active muscle contraction, with larger *c* values indicating faster rates of cross-bridge detachment or reductions in myosin attachment time [$t_{on} = (2\pi c)^{-1}$] (27). The fastest rates of cross-bridge force production and detachment occurred at 0.78% Dextran T-10, showing an ~150% increase in $2\pi b$ and 65% decrease in t_{on} compared to the slowest cross-bridge transition rates at 20% T-10 (Table 2). These shifts in cross-bridge rates of force development and detachment were consistent with trends observed for the frequency shifts for maximal work and power output.

DISCUSSION

We investigated the structural and functional relationships between myofilament lattice spacing and protein hydration on myosin-actin cross-bridge kinetics by examining the differential effects of two osmolytes; one is excluded from the myofilament lattice (Dextran T-500) and the other freely diffuses into the lattice (Dextran T-10). A critical component of this study was the use of small angle XRD to measure the in vitro myofilament lattice spacing in dissected IFM fibers to compare with the in vivo spacing from live fruit flies. Our results indicate that a structural change in the thick-to-thin filament surface distance plays a dominant role in dictating cross-bridge cycling rates, specifically cross-bridge attachment time (t_{on}). As discussed below, these findings illustrate a structural mechanism that may underlie variations in cross-bridge rates of force development and detachment throughout a contraction-relaxation cycle in striated muscle.

Thick-to-thin filament surface distance alters cross-bridge cycling rates

Cross-bridge kinetics were different (Tables 1 and 2) at matched values of inter-thick filament lattice spacing (4 and 6% T-500 vs. 10 and 20% T-10) and shifted in opposite directions for T-500 versus T-10 at matched values of myofilament protein hydration (4 and 6% T-500 vs. 0.34 and 0.78% T-10). Together these data show that neither center-to-center inter-thick filament lattice spacing nor myofilament protein hydration is solely responsible for altering cross-bridge rates of force development or detachment. As increasing osmotic pressure also decreases myofilament protein hydration, we posit a concomitant structural change in the thick filament backbone. We further hypothesize that thick-to-thin filament surface-to-surface distance ($d_{thick\text{-}thin}$), rather than center-to-center inter-thick filament spacing ($d_{inter\text{-}thick}$), is the relevant structural variable eliciting alterations in cross-bridge transition rates under modest osmotic pressures.

To test this hypothesis we developed a structural model, as $d_{thick\text{-}thin}$ cannot be directly obtained from XRD patterns of *Drosophila* IFM. The effect of Dextran on $d_{inter\text{-}thick}$ was

TABLE 2 Model parameter values for fits to Eq. 2 (mean ± SE)

Dextran concentration	A	*k*	B	*b*	C	*c*	t_{on}	
(wt/vol)	(kN m^{-2})	(unitless)	(kN m^{-2})	(Hz)	(kN m^{-2})	(Hz)	(ms)	(*n*)
0% T-500	138 ± 15	0.114 ± 0.004	1741 ± 175	271 ± 7	1600 ± 170	323 ± 6	0.49 ± 0.01	10
4% T-500	151 ± 18	0.118 ± 0.004	2287 ± 393	206 ± 6*	2188 ± 383	244 ± 5*†	0.65 ± 0.01*†	10
6% T-500	150 ± 20	0.119 ± 0.004	2059 ± 362	189 ± 4*	1986 ± 356	224 ± 3*†	0.71 ± 0.01*†	10
0% T-10	143 ± 11	0.114 ± 0.003	2101 ± 286	276 ± 5	1965 ± 278	320 ± 5	0.50 ± 0.01	11
0.34% T-10	141 ± 12	0.116 ± 0.003	1956 ± 270	290 ± 6*	1820 ± 261	340 ± 6*	0.47 ± 0.01*	11
0.78% T-10	134 ± 11	0.114 ± 0.003	1559 ± 7	307 ± 7*	1438 ± 7	363 ± 5*‡	0.44 ± 0.01*	9
10% T-10	122 ± 13	0.123 ± 0.010	1497 ± 8	153 ± 4*†‡	1500 ± 8	183 ± 5*†‡	0.88 ± 0.03*†‡	11
20% T-10	140 ± 11	0.152 ± 0.007*	2172 ± 270	110 ± 4*†‡	2133 ± 281	125 ± 4*†‡	1.29 ± 0.04*†‡	11

*Differs from 0% Dextran value within the population of T-10 or T-500 measurements using a linear mixed model with Dextran concentration as the repeated measure followed by a pairwise comparison of the means ($p < 0.05$).

†Differs from all other values within the population of T-10 or T-500 measurements using a linear mixed model with Dextran concentration as the repeated measure followed by a pairwise comparison of the means ($p < 0.05$).

‡Differs from all other values among the entire population of measurements using a 1-way ANOVA followed by a multiple comparison of means ($p < 0.05$).

calculated using linear fits to our x-ray measurements after averaging the intercept values (Fig. 1 *A*):

$$d_{inter\text{-}thick}(T\text{-}500) = 61.575\text{-}1.47[\%\text{T-}500],$$
$$d_{inter\text{-}thick}(T\text{-}10) = 61.575\text{-}0.48[\%\text{T-}10]. \quad (3)$$

Using Eq. 3, $d_{inter\text{-}thick}$ increased 10.6% at 0% T-500 and decreased 5.3% at 6% T-500, compared to 4% T-500 (Fig. 4 *A*). Prior estimates from electron density maps and myofilament structure models in frog tissue (14) have shown that the thick filament backbone and myofilament lattice were compressed similarly as osmotic pressure increased (0–3 kPa), leading to our assumption of a 1:1 compression ratio for thick filament backbone compression to myofilament lattice compression for T-500. Given a 1:1 compression ratio and an in vivo value of 8 nm (28), the radius of the thick filaments (r_{thick}) would increase 10.6% to 8.8 nm at 0% T-500 and decrease 5.3% to 7.6 nm at 6% T-500 (Fig. 4 *B*).

Thus, $d_{thick\text{-}to\text{-}thin}$ is

$$d_{thick-to-thin} = \frac{d_{inter\text{-}thick}}{2} - (r_{thick} + r_{thin}), \quad (4)$$

where $d_{inter\text{-}thick}/2$ represents the center-to-center distance between an adjacent pair of thin and thick filaments (Eq. 3) and r_{thin} is the thin filament radius set at the in vivo value of 4 nm (29), assuming an incompressible solid cylinder. These calculations predict that increasing osmotic pressure using T-500 reduces $d_{thick\text{-}to\text{-}thin}$ (Fig. 4 *C*) because the magnitude of $d_{inter\text{-}thick}$ decreases more than r_{thick} (Fig. 4, *A* and *B*). As discussed in detail in the Methods, we assume that matched osmotic pressures between Dextran T-500 and T-10 produce similar myofilament protein hydration conditions, based upon previous osmotic pressure studies (20,21). This matches values for r_{thick} between T-500 and T-10 at matched osmotic pressures. For example, r_{thick} for 0.34% T-10 and 4% T-500 are equal as these conditions produce identical osmotic pressures (Fig. 4 *B*). In contrast to the reduced $d_{thick\text{-}to\text{-}thin}$ predicted for increasing T-500, the model predicts increasingly greater values for $d_{thick\text{-}to\text{-}thin}$ at matched osmotic pressures for 0.34 and 0.78% T-10 (Fig. 4 *C*) because T-10 reduces r_{thick} by 5–10% without significantly reducing $d_{inter\text{-}thick}$.

This structural model resolves the seemingly divergent trends in cross-bridge cycling rates with increased osmotic pressure from T-500 and T-10, by demonstrating that the frequency of maximal power output and t_{on} are correlated with $d_{thick\text{-}to\text{-}thin}$ (Fig. 5). This finding indicates that the rates of cross-bridge force production and detachment decrease as the volume in which myosin operates decreases, and

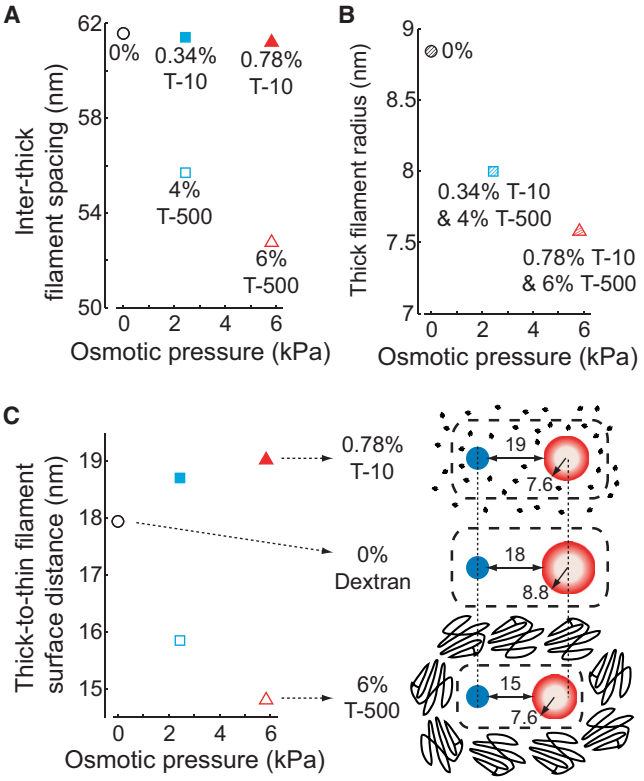

FIGURE 4 (A) Inter-thick filament spacing values for Dextran T-500 and T-10 were calculated from linear fits (Eq. 3) to x-ray diffraction measurements (Fig. 1) and plotted against osmotic pressure. (*B*) Reductions in thick filament radius with increased osmotic pressure were calculated from the fractional changes in inter-thick filament spacing with Dextran T-500, using an 8 nm in vivo thick filament radius (28) and a fixed thin filament radius of 4 nm (29). (*C*) The relationship between thick-to-thin filament surface distance and osmotic pressure was calculated (Eq. 4) from the values in panels *A* and *B*. The effects of osmotic stress on a pair of thin (*solid*) and thick (*hollow*) filaments are illustrated for 6% T-500 (*lower*), 0% Dextran (*middle*), and 0.78% T-10 (*upper*), with thick filament radius and thick-to-thin filament surface distance listed in nm. Dashed boxes outline myofilament lattice space, where Dextran T-10 diffuses into the lattice to reduce thick filament radii without significantly affecting lattice spacing and from which Dextran T-500 is excluded to simultaneously compress thick filament radii and inter-thick filament lattice spacing. Vertical dashed lines across panel highlight the centered-alignment of thin filaments and shifted alignment of thick-filaments.

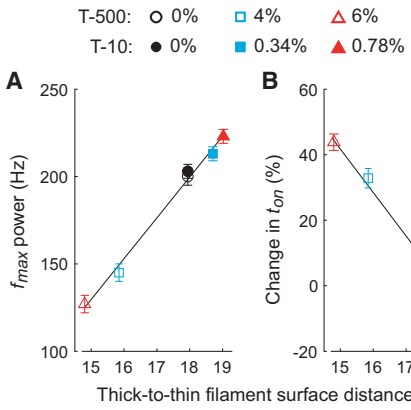

FIGURE 5 Frequency of maximal power (*A*) and percent changes in myosin attachment time, or t_{on}, (*B*) for Dextran T-500 and T-10 (*n* in Table 2), are plotted against modeled thick-to-thin filament surface distance from Fig. 4 *C*.

introduces a fundamental structural variable that strongly modulates contractile function in a muscle fiber. This agrees with previous measurements showing a high correlation between faster shortening velocity and increased thick-to-thin filament spacing (30) and remains consistent with reports of reduced ATP hydrolysis rate upon compressing muscle fibers to near in vivo spacing with Dextran T-500 (12,13,31). Although previous studies have correlated their results to the measured value of $d_{inter\text{-}thick}$ (7,10–13,32), our results suggest that myofilament diameter must also be taken into account, making $d_{thick\text{-}to\text{-}thin}$ the more important measure.

Implications for striated muscle function

Decreased thick-to-thin filament surface distance reduced the rate of cross-bridge force development and prolonged t_{on}, demonstrating that structural changes in the myofilament lattice may have important implications for striated muscle performance throughout a contraction-relaxation cycle. During each skeletal or cardiac muscle contraction in vertebrates, muscle fibers undergo significant changes in length (10–25% (33,34)) and lattice spacing according to an approximately constant volume relationship (35–37). As thick-to-thin filament surface distance varies proportionally with lattice spacing during sarcomere lengthening, the smallest thick-to-thin filament surface distance occurs at the longest sarcomere lengths. According to our results, t_{on} would become longer, thereby producing a slower contractile velocity at longer sarcomere lengths, as studies indicate that contractile velocity is limited by the rate at which cross-bridges detach (38,39). Prolonged t_{on} at longer sarcomere lengths could enhance cooperative thin filament activation by strongly bound cross-bridges, potentially augmenting cross-bridge recruitment and force production (32,40–42). Conversely, maximum thick-to-thin filament surface distance would occur at the shortest sarcomere lengths, resulting in a faster rate of cross-bridge force production and shorter t_{on} that could reduce the number of attached cross-bridges, thereby facilitating relaxation and promoting muscle relengthening at the end of a contraction.

Our findings that t_{on} increases as thick-to-thin surface distance decreases could result from the cross-bridge bearing a reduced load through its power stroke, possibly due to a reduced extension of myosin S-2 because the myosin is simply closer to its actin binding partner. This hypothesis is supported by measurements showing various cross-bridge transition rates respond differently to positive versus negative strain (43) and previous *Drosophila* experiments from our laboratory showing t_{on} increases with reduced cross-bridge load/strain due to fiber shortening (24). Thus, variations in thick-to-thin filament surface distance may represent a structural mechanism for influencing strain-dependent molecular processes during striated muscle contraction.

Effects of in vivo lattice spacing in IFM fibers

Adding 4% T-500 to skinned *Drosophila melanogaster* IFM fibers returned myofilament lattice spacing and, presumably, protein hydration to their in vivo values. Compared to the swollen lattice (0% T-500), this condition reduced center-to-center inter-thick filament spacing by 10%, oscillatory power by 27%, and cross-bridge rates of force development and detachment by 24–33%. These changes are consistent with our previous *Drosophila* study showing that N-terminal truncation and phosphorylation mutations in the regulatory light chain were greatly affected by osmotic compression back to in vivo lattice spacing values, making single fiber mechanics more similar to whole fly flight characteristics (10). Thus, performing experiments in skinned fibers without compensating for the structural changes in the myofilament lattice can significantly alter functional performance and the accompanying scientific conclusions. For instance, the wing beat frequency of *Drosophila melanogaster* is ~145–150 Hz at the temperature (15°C) of our mechanics experiments (44,45). The swollen lattice data would indicate the cross-bridge kinetics driving wing beat frequency are tuned to maximal work output, because the frequency of maximal work occurs at 143 Hz, whereas the frequency of maximal power occurs at 200 Hz. However, under in vivo osmotic conditions, cross-bridge cycling rates appear to be tuned to maximal power as its maximal frequency occurs at 145 Hz and the frequency of maximum work drops to 112 Hz. Therefore, by controlling for in vivo lattice geometry, our results show that cross-bridge cycling rates may be tuned for power output near wing beat frequency.

Model limitations and alternative interpretations

Model predictions of thick-to-thin filament surface distance ($d_{thick\text{-}to\text{-}thin}$) were calculated from i), fitted values to myofilament lattice compression measurements ($d_{inter\text{-}thick}$) as osmotic pressure increased (Fig. 1), and ii), the assumption that thick filament radius (r_{thick}) for Dextran T-500 and Dextran T-10 decreased similarly, in proportion to $d_{inter\text{-}thick}$ as osmotic pressure increased for Dextran T-500 (14). Unfortunately, we were unable to directly extract estimates of the thick filament structure from XRD patterns from the live fly or skinned fibers using the methodology applied to frog tissue (14). Because fruit fly thick filaments are approximately three times stiffer than vertebrate thick filaments (46), they could be less compressible than frog thick filaments. Therefore, we investigated the consequences of various values for the compression ratio used in our structural model by reducing the degree of thick filament backbone compression with respect to myofilament lattice compression (ranging from 0.25:1 to 1:1; Fig. S1). The overall predictions of our structural model were insensitive to the exact value of the compression ratio, demonstrating that

changes in thick-to-thin filament surface-to-surface spacing remain highly correlated with t_{on} as long as r_{thick} modestly decreases with increased osmotic pressure.

The model can also be used to examine how predictions of thick-to-thin filament surface distance might change if r_{thick} responded differently than expected for T-500 or T-10. Exploring various possibilities for both Dextrans (Fig. S2), ranging from no thick filament compression (0:1 compression ratio) to 50% greater thick filament compression than myofilament lattice compression (1.5:1 compression ratio), we find that t_{on} remains well correlated with thick-to-thin filament surface distance as osmotic pressure increases as long as T-10 recompresses the thick filament at least modestly (<0.5:1 compression ratio). Although we assume equal osmotic pressures from T-500 and T-10 produce similar r_{thick}, T-10 may decrease r_{thick} more than T-500 (>1:1 compression ratio) because T-10 may have a larger effect at the thick filament surface (which it can come in contact with) than T-500 may have at the myofibril surface (beyond which it cannot enter but can still exert an osmotic pressure). Notably, t_{on} correlates with thick-to-thin filament surface distance for all T-500 compression ratios, including no thick filament compression. Thus, our overall findings that thick-to-thin filament surface distance correlates with t_{on} remain unchanged even if T-500 and T-10 were to differentially affect the thick filament backbone.

Dextran T-10 is capable of reducing lattice spacing, but the biophysical mechanism by which this occurs may differ from T-500. Potentially, T-10 could reduce myofilament lattice spacing due to contamination from large Dextran particles that remain excluded from the myofilament lattice. This case is unlikely as the fraction of T-10 $\geq$ 20 kDa, and thereby excluded from the myofilament lattice (8), is negligibly small. Alternatively, T-10 may compress or dehydrate proteins in the myofibrillar matrix, such as M-band or Z-line proteins that hold and anchor the myofilaments (47,48), and thus, lead to reduced lattice spacing. Another mechanism could stem from decreases in thick filament backbone diameter that might lead to reduced myofilament lattice spacing (49). Either of these mechanisms could explain why lattice compression from T-10 requires much higher osmotic pressures than T-500 to match lattice spacing.

The lowest frequencies of maximal work and power occurred at the highest Dextran T-10 concentrations (10% and 20%), which could follow from i), high osmotic pressures deforming the myofilament proteins to diminish the actin-myosin interaction, or ii), T-10 molecules could be interfering with cross-bridge formation by being in the way of myosin binding to actin. We would not expect Dextran T-10 to significantly inhibit cross-bridge formation at low concentrations (0.34% and 0.78%), as previous studies using small Dextrans or PEG (13,15–17) have not suggested such interference.

CONCLUSIONS

These experiments coupled XRD measurements of myofilament lattice spacing in live fruit flies and skinned IFM fibers with mechanical measurements from skinned IFM fibers to differentiate the influence of myofilament lattice spacing versus myofilament protein hydration on cross-bridge cycling kinetics. Our measurements and modeling suggest that thick-to-thin filament surface spacing influences rates of cross-bridge force development and detachment more strongly than myofilament hydration. This study introduces a structural variable that may strongly dictate cross-bridge behavior throughout in vivo contraction in striated muscle.

SUPPORTING MATERIAL

Materials and Methods and Discussion sections, two figures, and references (50,51) are available at http://www.biophysj.org/biophysj/supplemental/S0006-3495(12)00875-2.

We thank Dr. V. Adrian Parsegian for helpful discussions on osmotic compression and protein hydration and Dr. Jim O. Vigoreaux for maintaining and supplying the fruit flies.

This study was supported by grants from the National Institutes of Health (AG-031303, AR-049425, T32 HL007647, 9 P41 GM103622-17, and 2P41RR008630-17) and National Science Foundation (DBI-0905830). Use of the Advanced Photon Source, an Office of Science User Facility operated for the U.S. Department of Energy (DOE) Office of Science by Argonne National Laboratory, was supported by the U.S. DOE under contract No. DE-AC02-06CH11357.

The content is solely the responsibility of the authors and does not necessarily reflect the official views of the National Institutes of Health.

REFERENCES

1. Lang, F. 2007. Mechanisms and significance of cell volume regulation. *J. Am. Coll. Nutr.* 26(5, Suppl):613S–623S.
2. Hoffmann, E. K., I. H. Lambert, and S. F. Pedersen. 2009. Physiology of cell volume regulation in vertebrates. *Physiol. Rev.* 89:193–277.
3. Parsegian, V. A., R. P. Rand, and D. C. Rau. 1995. Macromolecules and water: probing with osmotic stress. *Methods Enzymol.* 259:43–94.
4. Rand, R. P., V. A. Parsegian, and D. C. Rau. 2000. Intracellular osmotic action. *Cell. Mol. Life Sci.* 57:1018–1032.
5. Matsubara, I., and G. F. Elliott. 1972. X-ray diffraction studies on skinned single fibres of frog skeletal muscle. *J. Mol. Biol.* 72:657–669.
6. Godt, R. E., and D. W. Maughan. 1977. Swelling of skinned muscle fibers of the frog. Experimental observations. *Biophys. J.* 19:103–116.
7. Godt, R. E., and D. W. Maughan. 1981. Influence of osmotic compression on calcium activation and tension in skinned muscle fibers of the rabbit. *Pflugers Arch.* 391:334–337.
8. Kawai, M., J. S. Wray, and Y. Zhao. 1993. The effect of lattice spacing change on cross-bridge kinetics in chemically skinned rabbit psoas muscle fibers. I. Proportionality between the lattice spacing and the fiber width. *Biophys. J.* 64:187–196.
9. Miller, M. S., B. M. Palmer, …, D. W. Maughan. 2005. The essential light chain N-terminal extension alters force and fiber kinetics in mouse cardiac muscle. *J. Biol. Chem.* 280:34427–34434.
10. Miller, M. S., G. P. Farman, …, D. W. Maughan. 2011. Regulatory light chain phosphorylation and N-terminal extension increase cross-bridge binding and power output in *Drosophila* at in vivo myofilament lattice spacing. *Biophys. J.* 100:1737–1746.

11. Kawai, M., and M. I. Schulman. 1985. Crossbridge kinetics in chemically skinned rabbit psoas fibres when the actin-myosin lattice spacing is altered by dextran T-500. *J. Muscle Res. Cell Motil.* 6:313–332.
12. Krasner, B., and D. W. Maughan. 1984. The relationship between ATP hydrolysis and active force in compressed and swollen skinned muscle fibers of the rabbit. *Pflugers Arch.* 400:160–165.
13. Zhao, Y., and M. Kawai. 1993. The effect of the lattice spacing change on cross-bridge kinetics in chemically skinned rabbit psoas muscle fibers. II. Elementary steps affected by the spacing change. *Biophys. J.* 64:197–210.
14. Irving, T. C., and B. M. Millman. 1989. Changes in thick filament structure during compression of the filament lattice in relaxed frog sartorius muscle. *J. Muscle Res. Cell Motil.* 10:385–394.
15. Chinn, M. K., E. B. Getz, …, S. L. Lehman. 2003. Force enhancement by PEG during ramp stretches of skeletal muscle. *J. Muscle Res. Cell Motil.* 24:571–578.
16. Chinn, M. K., K. H. Myburgh, …, R. Cooke. 2000. The effect of polyethylene glycol on the mechanics and ATPase activity of active muscle fibers. *Biophys. J.* 78:927–939.
17. Highsmith, S., K. Duignan, …, J. Cohen. 1996. Osmotic pressure probe of actin-myosin hydration changes during ATP hydrolysis. *Biophys. J.* 70:2830–2837.
18. Vink, H. 1971. Precision measurements of osmotic pressure in concentrated polymer solutions. *Eur. Polym. J.* 7:1411–1419.
19. Millman, B. M., K. Wakabayashi, and T. J. Racey. 1983. Lateral forces in the filament lattice of vertebrate striated muscle in the rigor state. *Biophys. J.* 41:259–267.
20. Parsegian, V. A., R. P. Rand, and D. C. Rau. 2000. Osmotic stress, crowding, preferential hydration, and binding: a comparison of perspectives. *Proc. Natl. Acad. Sci. USA.* 97:3987–3992.
21. Rau, D. C., B. Lee, and V. A. Parsegian. 1984. Measurement of the repulsive force between polyelectrolyte molecules in ionic solution: hydration forces between parallel DNA double helices. *Proc. Natl. Acad. Sci. USA.* 81:2621–2625.
22. Irving, T. C., and D. W. Maughan. 2000. In vivo x-ray diffraction of indirect flight muscle from *Drosophila melanogaster. Biophys. J.* 78:2511–2515.
23. Farman, G. P., M. S. Miller, …, T. C. Irving. 2009. Phosphorylation and the N-terminal extension of the regulatory light chain help orient and align the myosin heads in *Drosophila* flight muscle. *J. Struct. Biol.* 168:240–249.
24. Tanner, B. C. W., Y. Wang, …, B. M. Palmer. 2011. Measuring myosin cross-bridge attachment time in activated muscle fibers using stochastic vs. sinusoidal length perturbation analysis. *J. Appl. Physiol.* 110:1101–1108.
25. Wang, Q., C. Zhao, and D. M. Swank. 2011. Calcium and stretch activation modulate power generation in *Drosophila* flight muscle. *Biophys. J.* 101:2207–2213.
26. Campbell, K. B., M. Chandra, …, W. C. Hunter. 2004. Interpreting cardiac muscle force-length dynamics using a novel functional model. *Am. J. Physiol. Heart Circ. Physiol.* 286:H1535–H1545.
27. Palmer, B. M., T. Suzuki, …, D. W. Maughan. 2007. Two-state model of acto-myosin attachment-detachment predicts C-process of sinusoidal analysis. *Biophys. J.* 93:760–769.
28. Goode, M. D. 1972. Ultrastructure and contractile properties of isolated myofibrils and myofilaments from *Drosophila* flight muscle. *Trans. Am. Microsc. Soc.* 91:182–194.
29. Huxley, H. E., A. Stewart, …, T. Irving. 1994. X-ray diffraction measurements of the extensibility of actin and myosin filaments in contracting muscle. *Biophys. J.* 67:2411–2421.
30. Riley, D. A., J. L. W. Bain, …, R. H. Fitts. 2005. Skeletal muscle fiber atrophy: altered thin filament density changes slow fiber force and shortening velocity. *Am. J. Physiol. Cell Physiol.* 288:C360–C365.
31. Myburgh, K. H., and R. Cooke. 1997. Response of compressed skinned skeletal muscle fibers to conditions that simulate fatigue. *J. Appl. Physiol.* 82:1297–1304.
32. Konhilas, J. P., T. C. Irving, and P. P. de Tombe. 2002. Length-dependent activation in three striated muscle types of the rat. *J. Physiol.* 544:225–236.
33. Guccione, J. M., W. G. O'Dell, …, W. C. Hunter. 1997. Anterior and posterior left ventricular sarcomere lengths behave similarly during ejection. *Am. J. Physiol.* 272:H469–H477.
34. Ahn, A. N., R. J. Monti, and A. A. Biewener. 2003. In vivo and in vitro heterogeneity of segment length changes in the semimembranosus muscle of the toad. *J. Physiol.* 549:877–888.
35. Yagi, N., H. Okuyama, …, F. Kajiya. 2004. Sarcomere-length dependence of lattice volume and radial mass transfer of myosin cross-bridges in rat papillary muscle. *Pflugers Arch.* 448:153–160.
36. Irving, T. C., J. Konhilas, …, P. P. de Tombe. 2000. Myofilament lattice spacing as a function of sarcomere length in isolated rat myocardium. *Am. J. Physiol. Heart Circ. Physiol.* 279:H2568–H2573.
37. Brandt, P. W., E. Lopez, …, H. Grundfest. 1967. The relationship between myofilament packing density and sarcomere length in frog striated muscle. *J. Cell Biol.* 33:255–263.
38. Siemankowski, R. F., M. O. Wiseman, and H. D. White. 1985. ADP dissociation from actomyosin subfragment 1 is sufficiently slow to limit the unloaded shortening velocity in vertebrate muscle. *Proc. Natl. Acad. Sci. USA.* 82:658–662.
39. Nyitrai, M., R. Rossi, …, M. A. Geeves. 2006. What limits the velocity of fast-skeletal muscle contraction in mammals? *J. Mol. Biol.* 355: 432–442.
40. Bremel, R. D., and A. Weber. 1972. Cooperation within actin filament in vertebrate skeletal muscle. *Nat. New Biol.* 238:97–101.
41. Fitzsimons, D. P., and R. L. Moss. 1998. Strong binding of myosin modulates length-dependent Ca2+ activation of rat ventricular myocytes. *Circ. Res.* 83:602–607.
42. Smith, L., C. Tainter, …, D. A. Martyn. 2009. Cooperative cross-bridge activation of thin filaments contributes to the Frank-Starling mechanism in cardiac muscle. *Biophys. J.* 96:3692–3702.
43. Ranatunga, K. W., M. E. Coupland, and G. Mutungi. 2002. An asymmetry in the phosphate dependence of tension transients induced by length perturbation in mammalian (rabbit psoas) muscle fibres. *J. Physiol.* 542:899–910.
44. Hyatt, C. J., and D. W. Maughan. 1994. Fourier analysis of wing beat signals: assessing the effects of genetic alterations of flight muscle structure in Diptera. *Biophys. J.* 67:1149–1154.
45. Swank, D. M., W. A. Kronert, …, D. W. Maughan. 2004. Alternative N-terminal regions of *Drosophila* myosin heavy chain tune muscle kinetics for optimal power output. *Biophys. J.* 87:1805–1814.
46. Miller, M. S., B. C. W. Tanner, …, J. O. Vigoreaux. 2010. Comparative biomechanics of thick filaments and thin filaments with functional consequences for muscle contraction. *J. Biomed. Biotechnol.* 2010: 473423.
47. Agarkova, I., and J. C. Perriard. 2005. The M-band: an elastic web that crosslinks thick filaments in the center of the sarcomere. *Trends Cell Biol.* 15:477–485.
48. Saide, J. D. 2006. The insect z-band. *In* Nature's Versatile Engine: Insect Flight Muscle Inside and Out. J. Vigoreax, editor. Landes Biosciences, Georgetown, TX. 150–166.
49. Farman, G. P., J. S. Walker, …, T. C. Irving. 2006. Impact of osmotic compression on sarcomere structure and myofilament calcium sensitivity of isolated rat myocardium. *Am. J. Physiol. Heart Circ. Physiol.* 291:H1847–H1855.
50. Godt, R. E., and B. D. Lindley. 1982. Influence of temperature upon contractile activation and isometric force production in mechanically skinned muscle fibers of the frog. *J. Gen. Physiol.* 80:279–297.
51. White, D. C. 1983. The elasticity of relaxed insect fibrillar flight muscle. *J. Physiol.* 343:31–57.

Supporting Material

Thick-to-thin filament surface distance modulates cross-bridge kinetics in Drosophila flight muscle

Bertrand C.W. Tanner[*], Gerrie P. Farman[†], Thomas C. Irving[‡],
David W. Maughan[*], Bradley M. Palmer[*], and Mark S. Miller[*]

* Department of Molecular Physiology and Biophysics, University of Vermont, Burlington, VT 05405. † Department of Physiology and Biophysics, Boston University, Boston, MA, 02118. ‡ Center for Synchrotron Radiation Research and Instrumentation, Department of Biological and Chemical Sciences, Illinois Institute of Technology, Chicago, IL 60616

Materials and Methods

Solutions: Solutions were prepared according to a computer program that solves the ionic equilibria (1). Concentrations are expressed in mmol/L (mM). Unless listed otherwise, all chemicals were purchased from Sigma-Aldrich (St. Louis, MO). Skinning solution was pCa 8.0 (pCa=-$\log_{10}[Ca^{2+}]$), 20 N,Nbis[2-hydroxyethyl]-2-aminoethanesulfonic acid (BES), 10 DTT, 5 EGTA, 1 Mg^{2+}, 5 MgATP, 0.25 P_i, protease inhibitor cocktail (Roche; Indianapolis, IN), ionic strength of 175 mEq adjusted with sodium methane sulfate, pH 7.0, with 50% w/v glycerol subsequently added and 0.5% Triton X-100. Storage solution was skinning solution without Triton. For x-ray diffraction measurements, relaxing solution was pCa 8.0, 20 BES, 15 creatine phosphate (CP), 300 U/mL creatine phosphokinase (CPK), 1 DTT, 5 EGTA, 1 Mg^{2+}, 15 MgATP, 8 P_i, ionic strength of 200 mEq adjusted with sodium methane sulfate at pH 7.0. For mechanics experiments, activating solution was pCa 4.0, 20 BES, 20 CP, 450 U/mL CPK, 1 DTT, 5 EGTA, 1 Mg^{2+}, 12 MgATP, 2 P_i, 200 mEq ionic strength, pH 7.0; and relaxing solution (used during fiber mounting) was same as activating solution except at pCa 8.0.

X-ray diffraction: Single dorsolongitudinal muscle fibers were isolated from thoraces of 2-3 day old female flies, demembranated in skinning solution for 1 hour at 4°C, clipped with aluminum T-clips, and transferred to storage solution at -20˚C until use. Within five days of dissection, fibers were transferred from storage solution to perfusion chambers filled with relaxing solution (0% Dextran) and secured between adjustable hooks. Fibers were visually stretched beyond just taut to approximate the fiber lengths used during mechanics experiments and placed in the path of the x-ray beam. Perfusion chambers had thin Mylar windows allowing x-rays to pass through the fibers and transmural ports allowing solution exchanges via syringe. The peak intensity, widths, and separations for the 1,0 and 2,0 equatorial reflections were estimated using a non-linear least squares fitting procedure (2). The separation of the 1,0 equatorial reflections was transformed into the distance between the lattice planes of the thick filaments ($d_{1,0}$), which was converted to center-to-center distance between thick filaments (= $d_{1,0} \times 2/\sqrt{3}$), yielding inter-thick filament spacing.

Muscle mechanics: Single IFM fibers were dissected and skinned as described above for x-ray diffraction measurements, split lengthwise to ~100 μm diameter to reduce the cross-sectional area, clipped with aluminum T-clips, lowered into relaxing solution, then mounted between a

silicon crystal strain gauge and piezoelectric motor. Fibers were stretched 5% from their just-taut length in 1% increments, waiting 1 minute between each stretch, activated to pCa 4.5 in the absence of Dextran, and stretched in 3% increments until oscillatory work production reached a stable maximum as measured via sinusoidal analysis. Following each 3% stretch, we waited 3-5 minutes for tension to relax and stabilize before applying the sinusoidal analysis. This protocol was required to accommodate the high stiffness and a relatively large contribution of passive tension to total active tension in IFM fibers (3). Activating solutions with increasing Dextran concentrations were exchanged to obtain 4 and 6% T-500 or 0.34, 0.78, 10, and 20% T-10. Following each activating solution change, fibers were shortened until slack, allowed to equilibrate for 5 minutes, then re-stretched until oscillatory work reached a stable maximum.

Statistical Analysis: To examine statistical trends among Dextran T-500 or T-10 measurements we applied a repeated-measures analysis with Dextran concentration as the repeated measure, followed by a Bonferroni adjusted pair-wise comparison of the means at each Dextran concentration. To examine inter-Dextran statistical differences between all measurements we applied a one-way ANOVA followed by a Tukey-Kramer multiple comparison of the means.

Discussion

Using electron density maps and myofilament lattice models of skinned skeletal muscle from frogs, Irving and Millman (2) showed that both myofilament lattice spacing and thick filament diameter decreased proportionally at modest osmotic pressures (0-3 kPa). Thus, we used a 1:1 ratio for thick filament compression to myofilament lattice compression to derive our structural model (Fig. 4). However, the stiffer thick filaments of fruit fly IFM may resist compression more than thick filament backbones of frog skeletal muscle, suggesting that a different compression ratio (*i.e.* <1:1) may be more appropriate for fly flight muscle.

To investigate the sensitivity of our structural model to different ratios of thick filament backbone compression with respect to myofilament lattice spacing compression, we reduced the effect of osmotic compression on thick filament radii (r_{thick}) by 1/2 (Fig. S1 A and C) and 1/4 (Fig. S1 B and D), without changing the effect of osmotic compression on the measured myofilament lattice spacing. These changes in the compression ratio value had a small effect, shifting 0% Dextran values to slightly larger distances for compression ratios of 0.5:1 (Fig. S1 A and C) to 0.25:1 (Fig. S1 B and D). There were no changes in the in vivo r_{thick} values at 4% T-500 and 0.34% T-10, as expected. For 6% T-500 and 0.78% T-10, these compression ratios shifted thick-to-thin filament surface distance to slightly smaller values. Across all these models, the relationships between cross-bridge kinetics and thick-to-thin filament surface distance varied, but maintained the important trends that T-10 increased and T-500 decreased thick-to-thin filament surface distance. Altogether, these results show that the structural model is relatively insensitive to the exact value chosen for the compression ratio between the thick filament backbone and the myofilament lattice as a whole.

Our findings that thick-to-thin filament surface distance dictates the rates of cross-bridge force development and detachment arise from the primary assumption that the thick filament radius (r_{thick}) decreases proportional to osmotic pressure, whether produced by T-500 or T-10. However, it remains possible that Dextran T-500 and T-10 could reduce thick filament backbone

dimensions differently at matched osmotic pressures. Therefore, we recast the model to illustrate a range of possibilities where T-500 and T-10 differentially affect thick filament backbone compression (Fig. S2). However, for this set of plots we assumed that skinning results in the same value for r_{thick} (*i.e.* starting from 8.8 nm at 0% Dextran for T-500 and T-10). This is a slightly different assumption than the assumption applied to the data of Fig. S1, where osmotic pressure had differential effects on thick filament backbone compression versus myofilament lattice compression. Fig. S2 illustrates that our primarily findings hold across a range of differential compression possibilities for T-500 and T-10, including the subset explored in Fig. S1. Specifically, t_{on} correlates with thick-to-thin filament surface distance for all T-500 compression ratios, including no thick filament compression (0:1 compression ratio). t_{on} correlates with thick-to-thin filament surface distance for any T-10 compression ratio greater than 0.15:1, the ratio that predicts a vertical line for t_{on} versus thick-to-thin filament surface distance.

References

1. Godt, R. E. and B. D. Lindley. 1982. Influence of temperature upon contractile activation and isometric force production in mechanically skinned muscle fibers of the frog. *J. Gen. Physiol.* 80:279–297.

2. Irving, T. C. and B. M. Millman. 1989. Changes in thick filament structure during compression of the filament lattice in relaxed frog sartorius muscle. *J. Muscle Res. Cell Motil.* 10:385–394.

3. White, D. C. 1983. The elasticity of relaxed insect fibrillar flight muscle. *J. Physiol.* 343:31–57.

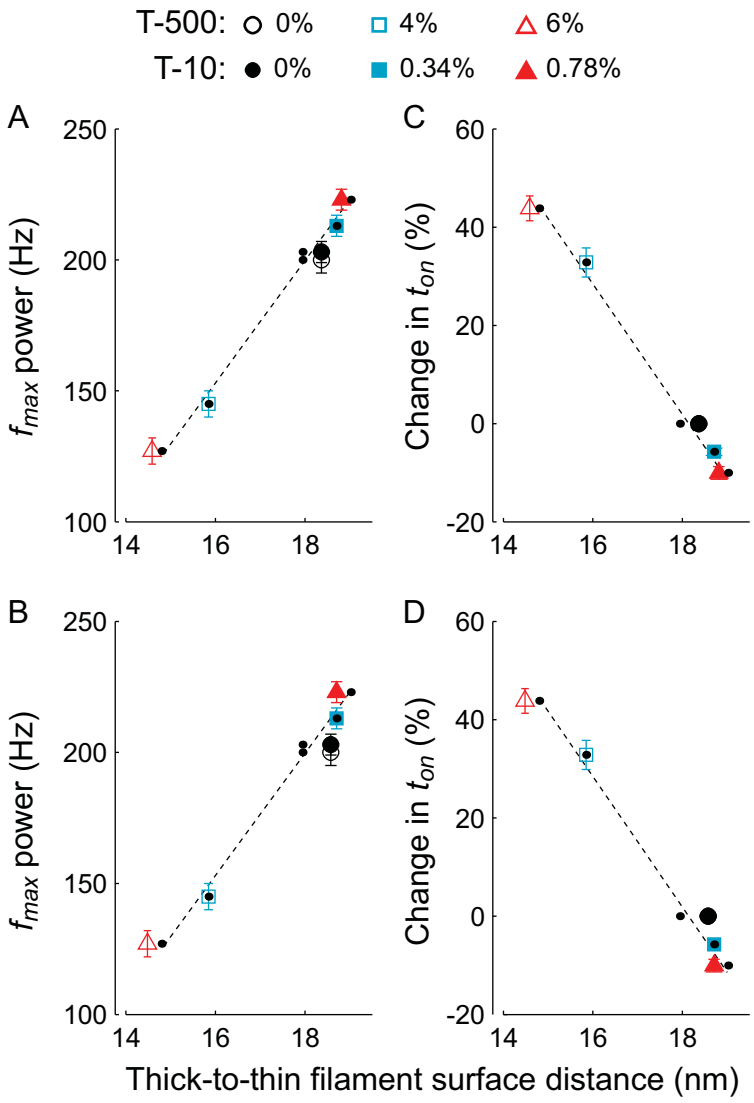

Figure S1: Frequency of maximal power (A and B) and myosin attachment time (C and D) are plotted against modeled thick-to-thin filament surface distance for thick filament backbone to myofilament compression ratios of 0.5:1 (A and C) and 0.25:1 (B and D). For reference, mean data and linear fits to the mean data from Fig. 5 are plotted as black dots and dashed lines to illustrate the 1:1 thick filament backbone to myofilament compression ratio presented in the main manuscript.

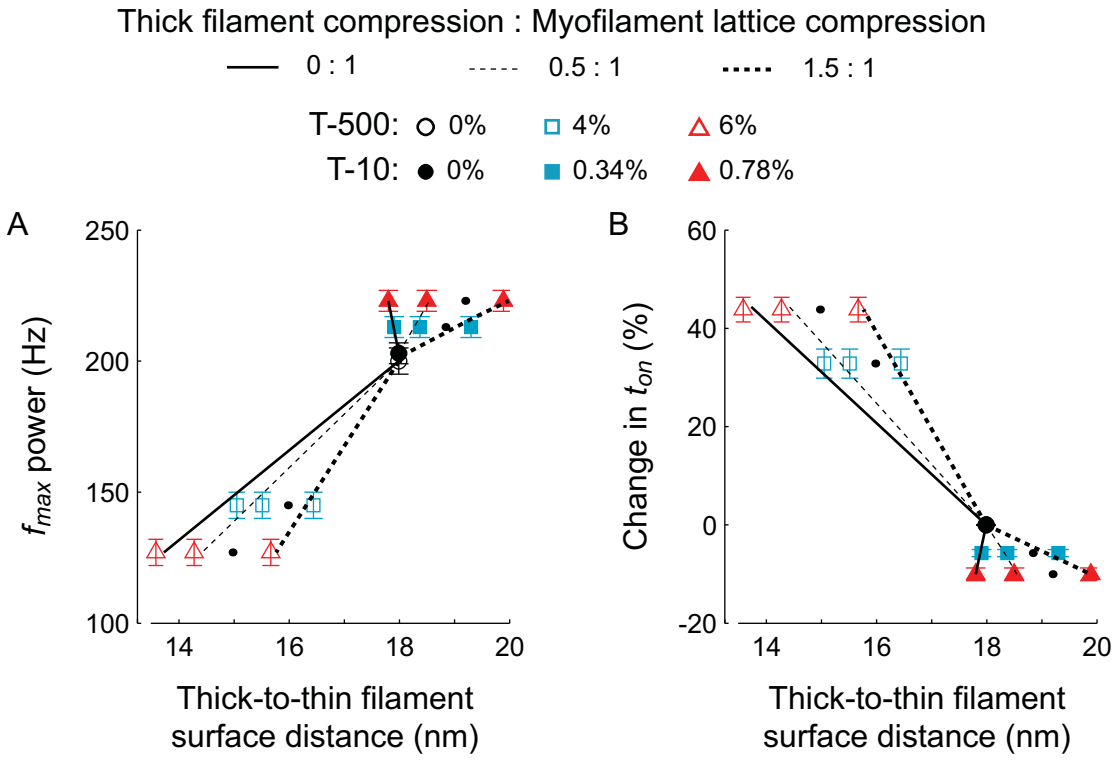

Figure S2: Frequency of maximal power (A) and change in myosin attachment time (B) are plotted against modeled thick-to-thin filament surface distance for conditions where i) T-500 and T-10 do not re-compress the thick filament backbone from the 0% Dextran condition (0:1 compression ratio), ii) Dextran T-500 and T-10 re-compress the thick filament backbone 50% less than the myofilament lattice (0.5:1 compression ratio), and iii) Dextran T-500 and T-10 re-compress the thick filament backbone 50% more than myofilament lattice (1.5:1 compression ratio). For reference, mean data from Fig. 5 are plotted as black dots to illustrate the 1:1 thick filament backbone to myofilament compression ratio presented in the main manuscript.